# Kinetics and mechanism of electron transfer in intact photosystem II and in the isolated reaction center: Pheophytin is the primary electron acceptor

A. R. Holzwarth[†‡], M. G. Müller[†], M. Reus[†], M. Nowaczyk[§], J. Sander[§], and M. Rögner[§]

[†]Max-Planck-Institut für Bioanorganische Chemie, Stiftstrasse 34-36, D-45470 Mülheim a.d. Ruhr, Germany; and [§]Lehrstuhl für Biochemie der Pflanzen, Ruhr-Universität Bochum, Universitätsstrasse 150, D-44801 Bochum, Germany

Edited by Charles J. Arntzen, Arizona State University, Tempe, AZ, and approved March 17, 2006 (received for review June 27, 2005)

**The mechanism and kinetics of electron transfer in isolated D1/D2-cyt$_{b559}$ photosystem (PS) II reaction centers (RCs) and in intact PSII cores have been studied by femtosecond transient absorption and kinetic compartment modeling. For intact PSII, a component of ≈1.5 ps reflects the dominant energy-trapping kinetics from the antenna by the RC. A 5.5-ps component reflects the apparent lifetime of primary charge separation, which is faster by a factor of 8–12 than assumed so far. The 35-ps component represents the apparent lifetime of formation of a secondary radical pair, and the ≈200-ps component represents the electron transfer to the $Q_A$ acceptor. In isolated RCs, the apparent lifetimes of primary and secondary charge separation are ≈3 and 11 ps, respectively. It is shown (*i*) that pheophytin is reduced in the first step, and (*ii*) that the rate constants of electron transfer in the RC are identical for PSII cores and for isolated RCs. We interpret the first electron transfer step as electron donation from the primary electron donor Chl$_{acc\ D1}$. Thus, this mechanism, suggested earlier for isolated RCs at cryogenic temperatures, is also operative in intact PSII cores and in isolated RCs at ambient temperature. The effective rate constant of primary electron transfer from the equilibrated RC* excited state is 170–180 ns$^{-1}$, and the rate constant of secondary electron transfer is 120–130 ns$^{-1}$.**

charge separation | photosynthesis | ultrafast spectroscopy | D1/D2-cyt$_{b559}$ | femtosecond absorption

Photosystem (PS) II cores, whose structure has recently been determined to a resolution of 3.5–3.2 Å (1–3), consist of the antenna polypeptides CP43 and CP47, which carry 13 and 16 chlorophyll (Chl) *a* molecules, respectively. They contain furthermore the D1/D2-cyt$_{b559}$ reaction center (RC) polypeptides, which bind the pigments of the electron transfer chain [four Chls, two pheophytins (Pheo), and two quinones] and two additional antenna Chls (the so-called Chl$_z^{D1}$ and Chl$_z^{D2}$ molecules). The isolated RC (D1-D2-cyt$_{b559}$) lacks the quinone acceptors and is thus only able to create a short-lived radical pair (RP) (see review in ref. 4).

There exists presently no agreement on the mechanism of the primary events of energy and electron transfer in the isolated RC complex (see refs. 4–6 for recent reviews). Early studies suggested an apparent ≈3-ps charge separation lifetime in the RC at room temperature (7, 8) in agreement with later studies (9, 10). Andrizhiyevskaya *et al.* (11) recently also proposed a model with an ≈3-ps charge separation. A somewhat slower charge separation of ≈8 ps has been reported by Wasielewski and coworkers (12), whereas more recent data from the same group were interpreted in terms of a 2- to 5-ps charge separation time (13). Substantially shorter charge separation times of 1 ps (14) and 0.4 ps (at 240 K) have been reported by Groot *et al.* (15). At the other extreme, a 1 order of magnitude longer charge separation time of ≈21 ps has been suggested by Klug and coworkers (16, 17). Probably the largest part of the controversial interpretations can be attributed to the lack of detailed kinetic and spectral modeling and not to actual major differences in the data. However, such modeling has been carried out only in few cases so far (9–11, 14, 18), whereas the important species-associated spectra (SAS) or species-associated difference spectra (SADS) of the intermediates have been calculated for even fewer cases (9, 14, 19).

A similarly controversial discussion concerns the question of whether the rates, and also the mechanism, of the early electron transfer processes in intact PSII cores and in isolated RCs are identical or not. Although we found very similar intrinsic rate constants for the primary charge separation in intact PSII cores (18) and in isolated D1/D2-cyt$_{b559}$ RCs (9), and also supported by studies on CP47/RCs (11), the identity of the electron transfer mechanism and the rates in intact PSII and RCs has been questioned recently (20–23) (for recent reviews see refs. 4, 24, and 25). In one publication, in fact, a difference in the primary charge separation rate of 2 orders of magnitude was claimed for the two systems (20). Thus, not only the kinetics but also the mechanism of electron transfer and the sequence of RPs in intact PSII RCs needs clarification.

The energy transfer and charge-separation kinetics in intact PSII cores was studied ≈2 decades ago by time-resolved fluorescence and transient absorption with a resolution of ≈10 ps (18, 26, 27). Dominant lifetime components with open RCs in the range of 35 (26) to 60–80 ps (27) were assigned to antenna energy trapping by primary charge separation, whereas a 200- to 500-ps lifetime was assigned to secondary electron transfer to the quinone acceptor $Q_A$ (18, 26, 27). The primary RP was assumed to be $P680^+Pheo^-$. These data subsequently gave rise to the development of a kinetic model for the energy and electron transfer processes in PSII cores known as the "exciton/RP equilibrium (ERPE) model" (18). The ERPE model assumed that energy equilibration between the core antenna and the RC occurs on a time scale of a few picoseconds (18), i.e., below the ≈10-ps resolution of the kinetic experiments at that time. However, on the basis of the x-ray data showing the relatively large distance of the antenna Chls to the RC pigments of ≈25 Å (1), it has been questioned that energy equilibration between antenna and RC should be faster than overall charge separation (6, 20, 21). These authors concluded that energy transfer to the RC was severely limiting the overall charge separation (trapping) process and proposed a "transfer-to-the-trap limited" model. If correct, this situation would have severe consequences for our understanding of the overall mechanism of charge separation.

Conflict of interest statement: No conflicts declared.

This paper was submitted directly (Track II) to the PNAS office.

Freely available online through the PNAS open access option.

Abbreviations: PS, photosystem; Chl, chlorophyll; Pheo, pheophytin; RC, reaction center; SADS, species-associated difference spectrum; LFD, lifetime density; RP, radical pair; SE, stimulated emission.

‡To whom correspondence should be addressed. E-mail: holzwarth@mpi-muelheim.mpg.de.

We showed recently that in isolated D1-D2-cyt$_{b559}$ complexes at low temperature, the primary electron donor is Chl$_{acc\ D1}$ (where acc is accessory), and we hypothesized that the primary electron acceptor should be Pheo$_{D1}$ (28). This mechanism also got support later on the basis of steady-state spectroscopy on mutant RCs (29), by theoretical calculations (30, 31), and by hole burning (32). However, this mechanism has neither been experimentally confirmed so far in time-resolved experiments at ambient temperatures for isolated RCs nor for intact PSII particles. The present work provides a previously unreported comparison of the electron transfer mechanisms for isolated RCs and intact PSII cores based on high-quality transient absorption data. The results provide experimental evidence for Pheo to be the primary electron acceptor in both samples.[¶] Based on the equality of the rate constants of the initial electron transfer steps, it is suggested that the same mechanism of electron transfer operates in the two systems.

## Results

**Isolated D1-D2 RCs.** Fig. 5 *A* and *B*, which is published as supporting information on the PNAS web site, shows the original transient absorption surfaces for $\lambda_{exc}$ = 681 nm before binning in the $Q_y$ range and in the critical low signal range of the Pheo $Q_x$ band, respectively. Inspection of the corresponding lifetime density (LFD) maps (cf. Fig. 1) shows that (*i*) several well separated lifetime distributions with peaks ranging from ≈100 fs to >5 ns appear, and (*ii*) that similar lifetime distributions, occasionally varying in their widths, occur in all wavelength ranges. A qualitative analysis is given in Table 1, which is published as supporting information on the PNAS web site. The experimental kinetics at some particularly informative detection wavelengths are shown in Fig. 6, which is published as supporting information on the PNAS web site.

We identified at least seven lifetime distribution peaks in the LFD maps. In all wavelength ranges, the widths of most of the lifetime distributions are relatively narrow. Pronounced exceptions are the 600- to 630-nm and 670- to 700-nm wavelength ranges for the 7- to 12-ps distribution. Thus, our data clearly exclude a very pronounced dispersion in the rates of the majority of the reaction steps but would be consistent with a modest dispersion in perhaps a few rates. Pronounced dispersive kinetics has been invoked in some papers to explain the rather complex overall kinetics (34–37). A huge dispersion for the rate of the primary charge separation (yielding lifetimes from 1 ps to 1 ns) has so far clearly been demonstrated only at low temperatures (10, 28, 32).

***Bleaching of the Pheo $Q_x$ band and decay of stimulated emission (SE).*** A weak spectral feature with positive amplitude extends from ≈540 to 590 nm (Fig. 1*B*). In particular signals in the 540–550 nm range indicates the reduction of the active Pheo $Q_x$ band but also the decay of the Pheo* state. It is important to note that the lifetime range below the 2–4 ps band is completely empty (Fig. 1*B*), with the exception of the 100- to 200-fs signal, which, however, has the wrong sign for the expected Pheo$^-$ rise. We thus qualitatively assign the reduction of the active Pheo, as indicated by the bleaching of the $Q_x$ band at 543 nm, and thus also the primary charge-separation step, to the lifetime distribution of 2–4 ps, peaking at 3 ps. The same lifetime(s) are present in the decay of SE >695 nm, whereas no significant SE decay can be seen at <2 ps down to 100 fs. We note that primary charge separation results in decay of excited states and thus must inevitably be accompanied by loss of SE. All these qualitative features suggest that (*i*) primary charge separation occurs with an apparent lifetime of 2–4 ps, (*ii*) that Pheo is the primary electron acceptor, and (*iii*) that any shorter-lived significant charge separation can be excluded. An ≈600-fs lifetime has very small amplitude and is observed only near 670 nm (Fig. 1*A*). It has been assigned to the slow phase of energy equilibration in the RC core (38), and our data support that interpretation. Two lifetime distributions of 30–50 ps and ≈100 ps in the 540–550 nm range are indicative of additional slower Pheo reduction phases, possibly limited by slow energy transfer from the peripheral Chl$_z$. This interpretation is supported also by a large amplitude of the 30- to 50-ps phase in the range >690 nm, indicating decay of SE and concomitant rise of absorption by formation of RPs (cf. Fig. 1*A*).

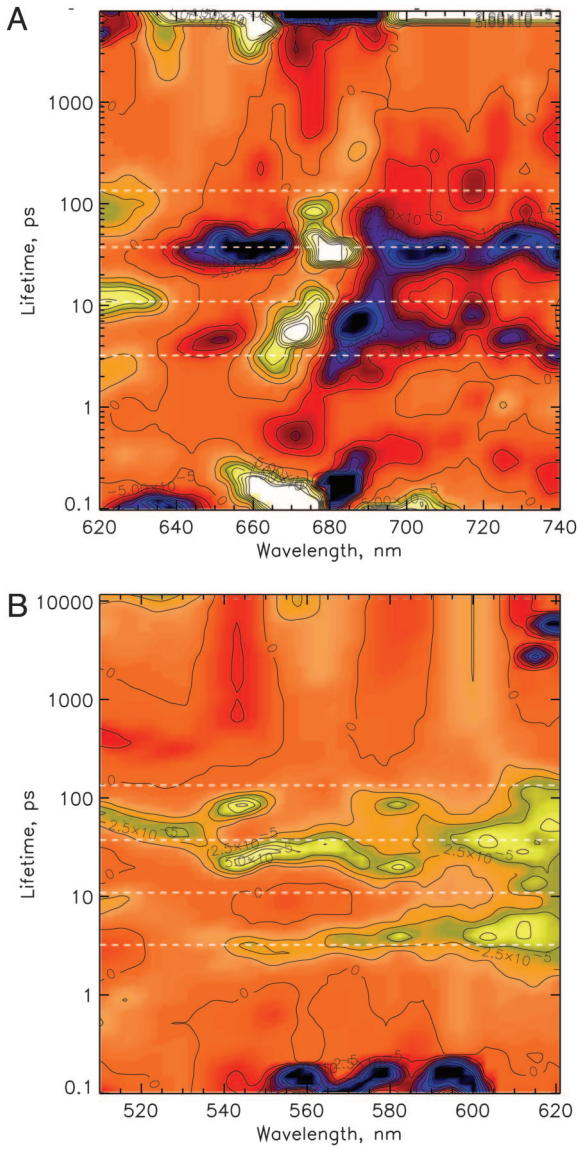


**Fig. 1.** LFD maps of the transient absorbance changes in the $Q_y$ (*A*) and the $Q_x$ (*B*) ranges of the chlorins in the isolated D1-D2 RC (excitation at 681 nm). The lifetimes are shown on a logarithmic scale. Yellow indicates positive amplitudes reflecting either the rise of a bleaching or the decay of an absorption; blue indicates negative amplitudes reflecting either the decay of a bleaching or the rise of an absorption. The dashed lines in the LFD maps represent the lifetimes obtained from the kinetic models.

***Kinetics in the chlorin $Q_y$ absorption band.*** Large-amplitude components in the range 660–700 nm are observed with lifetimes of 100–200 fs, 7–11 ps, and 30–50 ps, whereas the 2- to 4-ps lifetime

[¶]After submission of this work, Groot *et al.* (33) reported a transient mid-IR study of isolated D1-D2 RCs concluding also that the primary acceptor is Pheo and the primary donor the accessory Chl. A comparison with our data and discussion of the model of Groot *et al.* is provided in *Supporting Text* and Fig. 4, which are published as supporting information on the PNAS web site.

component shows smaller intensity. It is noteworthy that an ≈20-ps component with pronounced amplitude, as reported in several papers (16, 39, 40) and assigned to the apparent lifetime of Pheo reduction kinetics, is observed neither in the Pheo $Q_x$ nor in the chlorin $Q_y$ region. This result supports our previous interpretation, which assigned the ≈20-ps component reported by Klug and coworkers (16, 17) to a mixture of several components with longer (up to 50 ps) and shorter (3–10 ps) lifetimes (9, 19).

In the $Q_y$ region, the only range where a clear assignment, and in particular the important distinction between excited states on the one hand and RP states on the other hand, can be made, is the region >690 nm. In that range we expect some weak SE from the excited states of all chlorins at early times and broad absorption increases from the RPs upon charge separation. The most pronounced contribution to the development of an absorption increase should result from $P680^+$ (41), but $Pheo^-$ and $Chl^-$, if present, also would show an increase (42). The SE signal crosses the zero line at 5-ps delay (Fig. 6*C*). At that time ≈1/3 of the total absorption increase in the 700–735 nm region has occurred. Most of the remaining 2/3 of the absorption increase occurs with lifetimes ranging from 7 up to 100 ps. At 711 nm where SE and excited-state absorption cancel, the signal can be taken as a pure absorption increase from the RPs. Their rise kinetics is dominated by components with lifetimes of 2–4 and 30–50 ps in addition to a small amplitude component in the 7–11 ps range (cf. Fig. 1). All of these observations again confirm that the fastest component of charge separation is reflected in the lifetime distribution centered at ≈3 ps.

**Intact PSII Cores.** An excitation wavelength of 663 nm has been chosen to excite preferentially the blue absorbing part of the antenna complexes (cf. Fig. 7, which is published as supporting information on the PNAS web site, for original data). Fig. 2 shows the LFD maps for the $Q_y$ and the $Q_x$ ranges, respectively. Ignoring lifetimes below ≈500 fs, which reflect ultrafast spectral diffusion in the antenna, lifetimes with significant amplitudes are found in the range 0.5–1 and 1–2 ps forming an almost continuous broad lifetime distribution, 5–10 ps (small amplitudes), 35–40 ps, and ≈200 ps, besides a nondecaying component (>5 ns). The kinetics at two particularly informative wavelengths (SE at 701 nm and Pheo bleaching at 543 nm) together with the fitted signals (see below) are shown in Fig. 8, which is published as supporting information on the PNAS web site.

***Qualitative analysis of the kinetics and LFD maps.*** The fastest lifetime distribution (0.5–2 ps) clearly shows the features of an energy transfer process in the LFD map, and we assign it tentatively to energy transfer within the antenna complexes CP43 and CP47, in agreement with the equilibration lifetimes observed in the isolated complexes (43). The upper end of the distribution from 1–2 ps is assigned to antenna/RC equilibration (Fig. 2*A*). The origin of the 5- to 10-ps component(s) with smaller amplitudes is unclear and should be revealed by the kinetic model (see below). The large amplitude component (30–40 ps), dominated by a major loss of SE and rise of absorption >700 nm, can be assigned to the main trapping lifetime and reflects (secondary) RP formation. Another strong component with ≈200-ps lifetime is dominated by loss of bleaching around 680 nm and decay of absorption in the 640–660 nm range. In agreement with earlier data, this component can be assigned to electron transfer from $Pheo^-$ to $Q_A$ (26, 27). In the $Q_x$ range (Fig. 2*B*), two weak amplitude components in the range of 5–10 and ≈200 ps lifetime are observed around 540–550 nm, in addition to a much stronger amplitude component with a lifetime of 30–50 ps. These signals can be assigned qualitatively to the formation and decay of the $Q_x$ $Pheo^-$ bleaching band. The original kinetics in the range of the Pheo $Q_x$ band and in the SE/RP absorption region, respectively, are shown for two different time scales in Fig. 8.

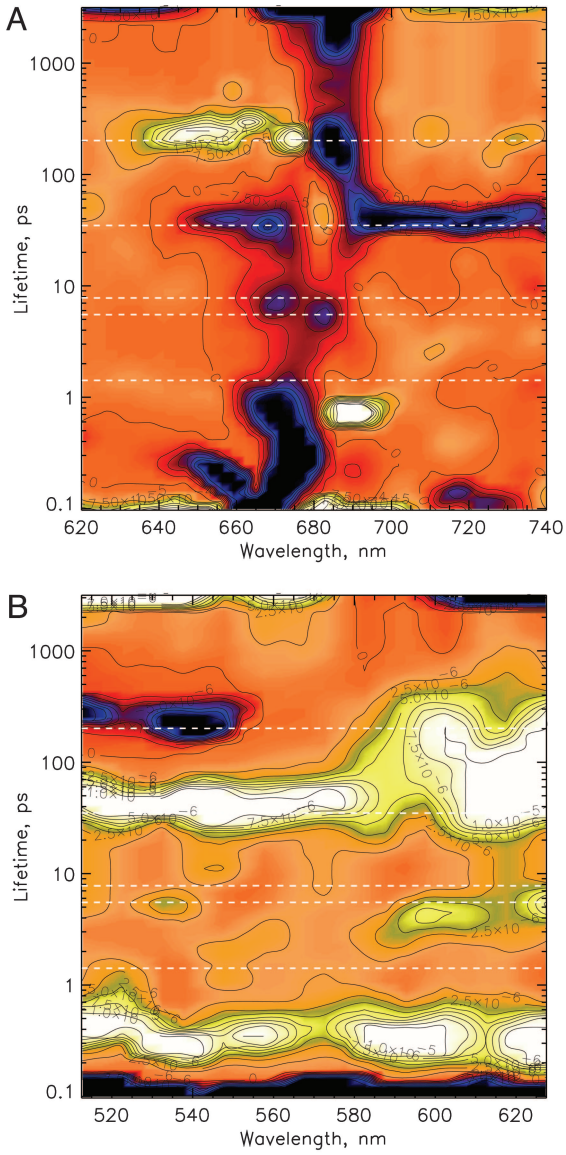


**Fig. 2.** LFD maps of the transient absorbance changes in the $Q_y$ (*A*) and the $Q_x$ (*B*) ranges of the chlorins in the PSII core (excitation at 663 nm). Presentation and color coding are the same as in Fig. 1.

***Kinetic models.*** As pointed out above, the LFD maps essentially show only a small number of relatively well defined lifetimes, which is a good basis for applying kinetic compartment modeling (44). We note that the apparent lifetimes are the negative inverse eigenvalues of the kinetic matrix and are thus functions of all rate constants in the scheme.

**Isolated D1-D2 RCs.** The minimal kinetic model sufficient to describe the data well comprises an excited RC* state, a compartment for the peripheral $Chl_z^*$, and three RP compartments. Any simpler models (less than five states) did not result in a satisfactory fit to the data. Because no charge separation occurs at <1-ps lifetime (see above), we include all lifetimes >1 ps in our kinetic modeling. Similar models have been proposed in our earlier work (9). Fitting the five-state model to the data results in lifetimes of 3.2, 11, 37, and 135 ps and ≥10 ns (Fig. 3*A*). As can be deduced from the eigenvectors corresponding to these lifetimes (see Fig. 9*B*, which is published as supporting information on the PNAS web site), the 3.2-ps lifetime reflects the

BIOPHYSICS

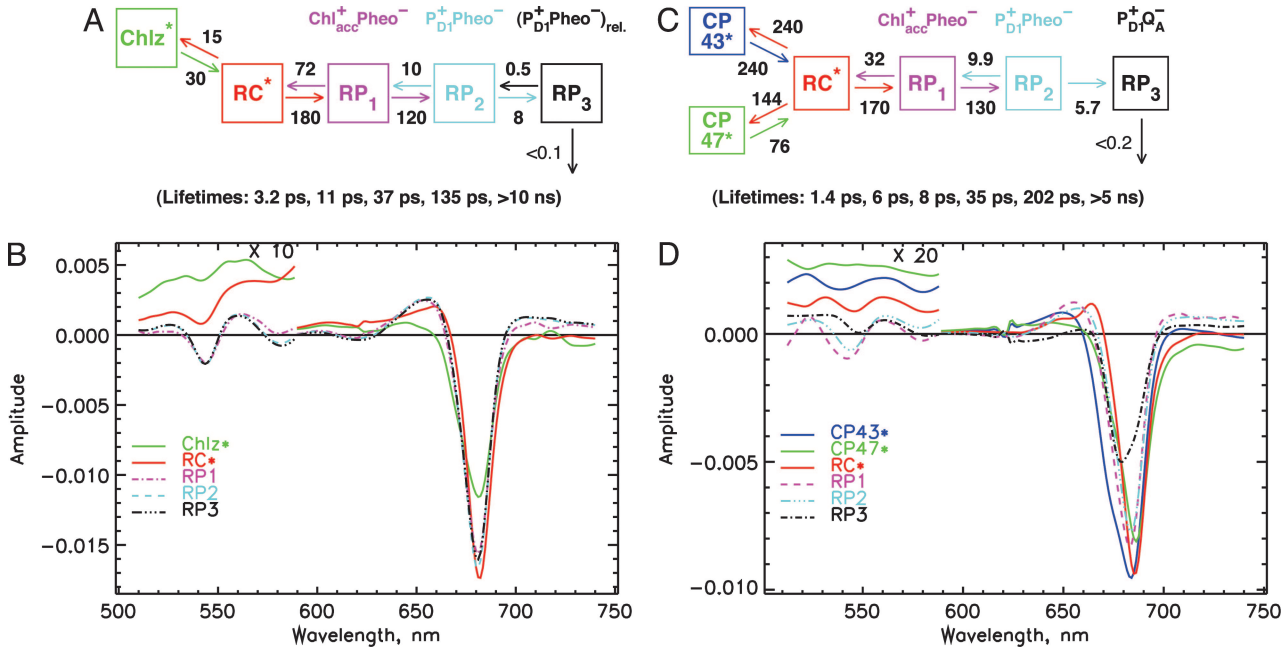


**Fig. 3.** Kinetic compartment models and SADS for isolated RC (*A* and *B*) and the intact PSII core (*C* and *D*). (*A* and *B*) Kinetic model with rate constants ($ns^{-1}$) and resulting lifetimes (bottom of image) (*A*) and corresponding SADS (note the change in scale near 590 nm) (*B*) for the isolated D1-D2 RC. (*C* and *D*) Kinetic model with rate constants ($ns^{-1}$) and resulting lifetimes (bottom) (*C*) and the corresponding SADS (note the change in scale near 590 nm) (*D*) for the intact PSII cores. The rate constants have an estimated error of ≈15%.

apparent primary charge separation lifetime, in agreement with our qualitative analysis given above. The 11-ps component reflects the apparent lifetime of secondary electron transfer, the 37-ps component reflects the energy equilibration time of the peripheral $Chl_z$ molecules with the RC, and the 135-ps component reflects the RP relaxation. The rate constant of primary charge separation from the equilibrated RC* state is 180 $ns^{-1}$, and the rate constant of secondary charge transfer is 120 $ns^{-1}$. The bleaching maximum of the RC* is located at 682 nm, whereas the RP states have bleaching maxima at 681 nm (Fig. 3*B*).

**Intact PSII Cores.** To avoid complicating the model too much we ignore, the ultrafast intra-antenna energy transfer processes, which are expected to give rise to main lifetimes in the 200 fs to 1 ps range (43). However, the model needs to include the effective rates of energy transfer between antenna and RC pigments on the one hand and the electron transfer rates in the RC on the other hand. In this minimal model, we do not consider any intra-RC energy transfer processes that occur well below 1 ps (see above). We thus include only the components >1 ps lifetime in our model, which is sufficient to answer the questions raised above. In view of the fact that the CP43 and CP47 antenna complexes are located on opposite sides of the RC and do have quite different spectra (43) and thus also different average energy transfer rates with the RC, the simplest compartment model that can be envisaged comprises two antenna compartments (one each for CP43 and CP47), one compartment for the excited equilibrated RC* (comprising the six chlorins in the RC), and two or more compartments for the different RPs. The results of fitting such a model to the data are shown in Fig. 3 *C* and *D*. The resulting model lifetimes are 1.4, 5.5, 7.8, 35, and 202 ps and >5 ns. The effective rate constants of energy transfer[‖] between antennae and RC are in the range 76–240 $ns^{-1}$ (cf. Fig. 3*C*). Thus, the 1.4-ps lifetime component describes the main ''apparent lifetime'' of the antenna/RC energy equilibration. The effective rate constant for primary electron transfer from the equilibrated RC* state to RP1 is 170 $ns^{-1}$, with a reverse transfer rate of 32 $ns^{-1}$. Secondary electron transfer to RP2 occurs also with a relatively high rate constant of 130 $ns^{-1}$, whereas electron transfer to RP3 proceeds with a rate constant of ≈5.7 $ns^{-1}$. The electron transfer between RP1 and RP2 is also reversible. The SADS shown in Fig. 3*D* show SE >720 nm for compartments 1–3 which is clearly characteristic for excited states, in agreement with the assignment of these compartments to CP43*, CP47*, and RC*. The CP43 compartment shows a significant shoulder on the blue side of the SADS around 670 nm as expected (43), whereas CP47 has a significantly narrower spectrum lacking most of the blue shoulder. CP43 shows the bleaching maximum at 683 nm and pronounced excited-state absorption near 650 nm, whereas the CP47 bleaching maximum is located at 686 nm. The SADS of the RC* is substantially narrower than the antenna SADS, showing a negative peak at 686 nm, and a pronounced excited state absorption around 665 nm, characteristic for a transition to the two-exciton band of the excitonically coupled RC complex. The SADS of all of the excited state compartments also show significant absorption in the 500–600 nm range (Fig. 3*D*). In contrast, the SADS of compartments 4–6 show the clear characteristics of RP states, best characterized by their broad absorption at >700 nm. They also show bleaching (≈540 nm) or very weak absorption in the 500–600 nm range. In the 650–700 nm range the SADS of RP1 and RP2 are very similar, showing the bleaching peak at 682 nm, i.e., 2-nm red-shifted relative to the corresponding SADS in the isolated RC. The SADS of RP3 shows a much smaller bleaching amplitude than RP1 and RP2 with a bleaching maximum at 680 nm. These properties of RP3 are characteristic for a decreased bleaching in the visible range because of electron transfer from $Pheo^-$ to $Q_A$. Thus, RP3 should be assigned to the RP $P680^+Q_A^-$ (27) with the electron hole most likely located on chlorin $P_{D1}$ (29, 46), whereas RP1 and RP2 with larger bleaching amplitude contain two bleached chlorins.

[‖]See ref. 45 for a definition of kinetic terms such as ''apparent lifetime,'' ''effective rate constant,'' etc.

## Discussion

**Mechanism and Kinetics of Electron Transfer.** Of particular interest for an assignment of the nature of the RPs and the mechanism of electron transfer are the SADS in the range of 540–550 nm where the $Q_x$ band of the active Pheo is located (47). From the SADS in this region the result is clear: The $Q_x$ band of the active $Pheo_{D1}$ is already fully bleached in RP1, and this bleaching at ≈543 nm remains also in RP2 and RP3 for the isolated RC (Fig. 3*B*). For PSII cores (Fig. 3*D*), the Pheo $Q_x$ bleaching is present in RP1 and RP2, whereas it is absent in RP3. This result means that Pheo in the active branch ($Pheo_{D1}$) is the primary electron acceptor in both systems. It also remains reduced in RP2. RP3 is different for the two systems, as expected. In intact PSII cores, $Pheo^-$ is reoxidized by electron transfer to $Q_A$ with a rate constant of 5.7 $ns^{-1}$. This process is not possible in isolated RCs because of the lack of quinones. Thus, RP3 in the latter case represents a thermodynamically relaxed RP in the same redox state as RP2 (their spectra are essentially identical).

***Assignment of the nature of the RPs.*** In view of the above-mentioned findings, it seems reasonable to assign RP1 to a $Chl^+_{acc\,D1}/Pheo^-_{D1}$ state. This assignment is based on the two following arguments: (*i*) The reduction of Pheo in the first electron transfer step is clearly demonstrated by the data, and (*ii*) we have already shown by other methods that $Chl_{acc\,D1}$ is the primary electron donor in D1-D2-$cyt_{b559}$ RCs at low temperature (28). A direct ultrafast electron transfer from one of the previously assumed donors $P_{D1}$ or $P_{D2}$ to $Pheo_{D1}$ does not appear to be possible, given the large distance of >14 Å (48, 49). Note that for an effective rate constant of primary charge separation of 180 $ns^{-1}$ from the equilibrated RC* state, the actual intrinsic rate constant of charge separation from the excited primary donor should be larger by a factor of ≈3, given the relative population of ≈0.33 of the $Chl_{acc\,D1}$ excited state in equilibrium (31). This value yields an intrinsic rate constant of charge separation of ≈550 $ns^{-1}$. Such a high rate constant for an electron transfer over a distance of ≈14 Å appears to be extremely unlikely (50). RP2 in both samples corresponds to the RP that has been assumed previously as representing the first charge-separated state (4, 18). However, our data now show that it requires two electron transfer steps to reach that state. The identity of the rates for the two initial electron transfer steps as well as the similiarity of the spectra of the respective RP intermediates strongly suggest that both the nature and the sequence of the reached RPs is the same for isolated D1-D2 RCs and intact PSII cores. All these observations together with the fact that Pheo is reduced in the first step and that $P^+Pheo^-$ is reached in the second step lead to an assignment of RP1 as $Chl^+_{acc}Pheo^-$. This conclusion also has been drawn from a study on pigment-modified RCs (51).

Interestingly this mechanism of electron transfer for PSII is reminiscent of a very similar situation for intact PSI cores where $Chl_{acc}$ has also been found to be the primary electron donor (52, 53). This similarity poses the intriguing question of whether the RCs of oxygenic photosynthesis should be considered to be the "role model" for RCs, rather than the more intensively studied purple bacterial RCs (see the discussion in ref. 4).

It is interesting to examine further the SADS of the RC* state near 540 nm. There is a distinct negative feature (bleaching) in the signal, floating on top of the pronounced excited-state absorption for both systems (Fig. 3 *B* and *D*). If we subtract the excited-state absorption background and put the remaining bleaching in relation to the maximal bleaching in the RP states at that wavelength, we estimate that ≈15–20% of the Pheo $Q_x$ band is bleached in the RC* state. This result corresponds reasonably with the expected relative population of the active Pheo excited state in the equilibrated RC* state of ≈15% (1 pigment out of 6). The time-dependent populations of the intermediates are shown in Fig. 9*A* for the isolated RC and in Fig. 10*A*, which is published as supporting information on the PNAS web site, for the intact PSII cores.

***Spectra of the peripheral $Chl_z$ in the isolated RC.*** In our model, we have described the two peripheral $Chl_z$ molecules as a single compartment. The heterogeneous SADS shows, however, that the two $Chl_z$ should have substantially different spectra (Fig. 3*B*). The bleaching maximum occurs at 682 nm, but the SADS shows a pronounced shoulder at 670 nm, which likely represents the bleaching maximum of the second (short-wave) $Chl_z$. If the second $Chl_z$ shows a bleaching at 670 nm, it would imply a 12-nm absorption difference in their maxima. This result is in contrast to most previous data, which were interpreted as indicating ≈670-nm maxima for both peripheral Chls (31, 54, 55). In an analysis of steady-state absorption spectra, we had assigned the two $Chl_z$ absorptions to 668 and 678 nm at low temperature (56). More recent work also indicated the pronounced spectral asymmetry of the two peripheral $Chl_z$ (13, 57). Thus, the SADS for $Chl_z$ found here is in agreement with those data.

**Trap-Limited or Transfer-to-Trap-Limited Kinetics in Intact PSII?** As discussed above, the model shown in Fig. 3*C* for all of the compartments yields very reasonable SADS, which are in agreement with the properties expected for the various species, e.g., SE at long wavelengths for excited states and increased absorption for the RPs (cf. Fig. 3*D*). Furthermore, the resulting rate constants also appear to be internally consistent. For example, by using appropriate assumptions for the average energy levels and antenna sizes of the various compartments, the ratios of forward to backward energy transfer rates are in the expected range required for detailed balance. All of these properties lend strong support for the notion that the compartment model shown in Fig. 3*C* provides an accurate description of the major processes in intact PSII cores. We have resolved in intact PSII cores (*i*) the rate-limiting energy transfer process(es) between antenna and RC (1.5 ps apparent lifetime), (*ii*) the apparent lifetime for energy trapping by charge separation (6 ps), and (*iii*) a previously undescribed early RP intermediate. The data show clearly that Pheo is the primary electron acceptor. Interestingly, the resulting apparent primary charge-separation lifetime for formation of the first RP state is 8–10 times faster than believed (20, 27).

The energy equilibration between antenna and RC occurs with an apparent lifetime of 1.5 ps, a value consistent with that assumed in the derivation of the exciton/RP equilibrium model (18). The average lifetime for excited-state decay in the kinetic model is ≈50 ps. Even extreme up-scaling of the energy transfer rates in the model by a factor of 100 only reduces this average excited-state decay time to 42 ps, which implies that the average delivery time of excitation from the antenna to the RC is ≈8 ps, i.e., much shorter than the average antenna decay time. As can be seen from the calculated population curves in Fig. 10*A*, the RC* state reaches its maximal population at ≈4.5 ps, whereas the RP1 state reaches its maximal population at ≈10 ps and RP2 at ≈80 ps after excitation. We conclude that energy delivery to the RC does not represent a bottleneck for the overall excited-state decay. Thus, despite the high intrinsic charge separation rate constant, the excited state decay in the PSII cores is overall trap-limited, in contrast to recent reports claiming an extreme transfer-to-the-trap limitation (6, 20, 21). This result confirms the assumptions of the early exciton/RP equilibrium model (27).

## Materials and Methods

Femtosecond transient absorption kinetics have been measured at room temperature on purified dimeric PSII core particles from *Thermosynechococcus elongatus* with intact oxygen evolution as reported in ref. 58 in a buffer of 20 mM Mes

BIOPHYSICS

(pH 6.5) and 200 mM mannitol. D1-D2-cyt$_{b559}$ RCs were isolated from spinach with a Chl/2 Pheo ratio of 6.2 ± 0.2 and were used for measurements under anaerobic conditions at 4°C as reported (19, 56). All samples were kept in a rotating (600 rpm) cuvette of 1-mm path length, which also was oscillated sideways with ≈60 rpm. The laser pulses from the optical parametric generator had a full-width at half-maximum of ≈120 fs, 6-nm spectral width, and a 3-kHz repetition rate. Multiple excitation of a particle has been avoided (absorbed photons per particle per pulse ≈ 0.1 for RCs and ≈0.35 for PSII cores). The kinetics are shown as LFD maps (see *Supporting Text* for a detailed explanation).

We thank Mrs. Iris Martin (Mülheim) for support in developing part of the data analysis software and Claudia König and Bettina Thüner (Bochum) for excellent technical assistance. This work was supported in part by European Union Human Resources and Mobility Activity Contract MRTN-CT-2003-505069 (to A.R.H.), the Higher Education and Scientific Research Office at Trento Province Project "Samba per 2", and Deutsche Forschungsgemeinschaft Grant SFB 480 (to M. Rögner).

1. Zouni, A., Witt, H. T., Kern, J., Fromme, P., Krauss, N., Saenger, W. & Orth, P. (2001) *Nature* **409,** 739–743.
2. Kamiya, N. & Shen, J.-R. (2003) *Proc. Natl. Acad. Sci. USA* **100,** 98–103.
3. Barber, J., Ferreira, K., Maghlaoui, K. & Iwata, S. (2004) *Phys. Chem. Chem. Phys.* **6,** 4737–4742.
4. Renger, G. & Holzwarth, A. R. (2005) in *Photosystem II: The Light-Driven Water: Plastoquinone Oxido-Reductase in Photosynthesis*, eds. Wydrzynski, T. & Satoh, K. (Springer, Dordrecht, The Netherlands), pp. 139–175.
5. Seibert, M. & Wasielewski, M. R. (2003) *Photosynth. Res.* **76,** 263–268.
6. Dekker, J. P. & van Grondelle, R. (2000) *Photosynth. Res.* **63,** 195–208.
7. Roelofs, T. A., Gilbert, M., Shuvalov, V. A. & Holzwarth, A. R. (1991) *Biochim. Biophys. Acta* **1060,** 237–244.
8. Holzwarth, A. R., Müller, M. G., Gatzen, G., Hucke, M. & Griebenow, K. (1994) *J. Luminesc.* **60 & 61,** 497–502.
9. Gatzen, G., Müller, M. G., Griebenow, K. & Holzwarth, A. R. (1996) *J. Phys. Chem.* **100,** 7269–7278.
10. Konermann, L., Gatzen, G. & Holzwarth, A. R. (1997) *J. Phys. Chem. B* **101,** 2933–2944.
11. Andrizhiyevskaya, E. G., Frolov, D., van Grondelle, R. & Dekker, J. P. (2004) *Phys. Chem. Chem. Phys.* **6,** 4810–4819.
12. Greenfield, S. R., Seibert, M., Govindjee & Wasielewski, M. R. (1997) *J. Phys. Chem. B* **101,** 2251–2255.
13. Wang, J., Gosztola, D., Ruffle, S. V., Hemann, C., Seibert, M., Wasielewski, M. R., Hille, R., Gustafson, T. L. & Sayre, R. T. (2002) *Proc. Natl. Acad. Sci. USA* **99,** 4091–4096.
14. van Mourik, F., Groot, M.-L., van Grondelle, R., Dekker, J. P. & van Stokkum, I. H. M. (2004) *Phys. Chem. Chem. Phys.* **6,** 4820–4824.
15. Groot, M.-L., van Mourik, F., Eijckelhoff, C., van Stokkum, I. H. M., Dekker, J. P. & van Grondelle, R. (1997) *Proc. Natl. Acad. Sci. USA* **94,** 4389–4394.
16. Hastings, G., Durrant, J. R., Barber, J., Porter, G. & Klug, D. R. (1992) *Biochemistry* **31,** 7638–7647.
17. Durrant, J. R., Hastings, G., Joseph, D. M., Barber, J., Porter, G. & Klug, D. R. (1993) *Biochemistry* **32,** 8259–8267.
18. Schatz, G. H., Brock, H. & Holzwarth, A. R. (1988) *Biophys. J.* **54,** 397–405.
19. Müller, M. G., Hucke, M., Reus, M. & Holzwarth, A. R. (1996) *J. Phys. Chem.* **100,** 9527–9536.
20. Vassiliev, S., Lee, C.-I., Brudvig, G. W. & Bruce, D. (2002) *Biochemistry* **41,** 12236–12243.
21. Vasil'ev, S., Orth, P., Zouni, A., Owens, T. G. & Bruce, D. (2001) *Proc. Natl. Acad. Sci. USA* **98,** 8602–8607.
22. Arsköld, S. P., Prince, B. J., Krausz, E., Smith, P. J., Pace, R. J., Picorel, R. & Seibert, M. (2004) *J. Luminesc.* **108,** 97–100.
23. Hughes, J. L., Prince, B. J., Krausz, E., Smith, P. J., Pace, R. J. & Riesen, H. (2004) *J. Phys. Chem. B* **108,** 10428–10439.
24. Diner, B. A. & Rappaport, F. (2002) *Annu. Rev. Plant Biol.* **53,** 551–580.
25. Holzwarth, A. R. (2004) in *Molecular to Global Photosynthesis*, eds. Archer, M. D. & Barber, J. (Imperial College Press, London), pp. 43–115.
26. Nuijs, A. M., van Gorkom, H. J., Plijter, J. J. & Duysens, L. N. M. (1986) *Biochim. Biophys. Acta* **848,** 167–175.
27. Schatz, G. H., Brock, H. & Holzwarth, A. R. (1987) *Proc. Natl. Acad. Sci. USA* **84,** 8414–8418.
28. Prokhorenko, V. I. & Holzwarth, A. R. (2000) *J. Phys. Chem. B* **104,** 11563–11578.
29. Diner, B. A., Schlodder, E., Nixon, P. J., Coleman, W. J., Rappaport, F., Lavergne, J., Vermaas, W. F. J. & Chisholm, D. A. (2001) *Biochemistry* **40,** 9265–9281.
30. Barter, L. M. C., Durrant, J. R. & Klug, D. R. (2003) *Proc. Natl. Acad. Sci. USA* **100,** 946–951.
31. Raszewski, G., Saenger, W. & Renger, T. (2005) *Biophys. J.* **88,** 986–998.
32. Riley, K., Jankowiak, R., Rätsep, M., Small, G. J. & Zazubovich, V. (2004) *J. Phys. Chem. B* **108,** 10346–10356.
33. Groot, M.-L., Pawlowicz, N. P., van der Wilderen, L. J. G. W., Breton, J., van Stokkum, I. H. M. & van Grondelle, R. (2005) *Proc. Natl. Acad. Sci. USA* **102,** 13087–13092.
34. Greenfield, S. R., Seibert, M., Govindjee & Wasielewski, M. R. (1996) *Chem. Phys.* **210,** 279–295.
35. Greenfield, S. R. & Wasielewski, M. R. (1996) *Photosynth. Res.* **48,** 83–97.
36. Donovan, B., Walker, L. A., Yocum, C. F. & Sension, R. J. (1996) *J. Phys. Chem.* **100,** 1945–1949.
37. Govindjee, van de Ven, M., Preston, C., Seibert, M. & Gratton, E. (1990) *Biochim. Biophys. Acta* **1015,** 173–179.
38. Durrant, J. R., Hastings, G., Joseph, D. M., Barber, J., Porter, G. & Klug, D. R. (1992) *Proc. Natl. Acad. Sci. USA* **89,** 11632–11636.
39. Klug, D. R., Rech, T., Joseph, D. M., Barber, J., Durrant, J. R. & Porter, G. (1995) *Chem. Phys.* **194,** 433–442.
40. Rech, T., Durrant, J. R., Joseph, D. M., Barber, J., Porter, G. & Klug, D. R. (1994) *Biochemistry* **33,** 14768–14774.
41. Allakhverdiev, S. I., Ahmed, A., Tajmir-Riahi, H. A., Klimov, V. V. & Carpentier, R. (1994) *FEBS Lett.* **339,** 151–154.
42. Fujita, I., Davis, M. S. & Fajer, J. (1978) *J. Am. Chem. Soc.* **100,** 6280–6282.
43. de Weerd, F. L., van Stokkum, I. H. M., van Amerongen, H., Dekker, J. P. & van Grondelle, R. (2002) *Biophys. J.* **82,** 1586–1597.
44. Holzwarth, A. R. (1996) in *Biophysical Techniques in Photosynthesis. Advances in Photosynthesis Research*, eds. Amesz, J. & Hoff, A. J. (Kluwer Academic, Dordrecht, The Netherlands), pp. 75–92.
45. Holzwarth, A. R., Müller, M. G., Niklas, J. & Lubitz, W. (2005) *J. Phys. Chem. B* **109,** 5903–5911.
46. Lubitz, W. (2002) *Phys. Chem. Chem. Phys.* **4,** 5539–5545.
47. Gounaris, K., Chapman, D. J., Booth, P. J., Crystall, B., Giorgi, L. B., Klug, D. R., Porter, G. & Barber, J. (1990) *FEBS Lett.* **265,** 88–92.
48. Ferreira, K. N., Iverson, T. M., Maghlaoui, K., Barber, J. & Iwata, S. (2004) *Science* **303,** 1831–1838.
49. Biesiadka, J., Loll, B., Kern, J., Irrgang, K.-D. & Zouni, A. (2004) *Phys. Chem. Chem. Phys.* **6,** 4733–4736.
50. Moser, C. C., Keske, J. M., Warncke, K., Farid, R. S. & Dutton, P. L. (1992) *Nature* **355,** 796–802.
51. Germano, M., Gradinaru, C. C., Shkuropatov, A. Y., van Stokkum, I. H. M., Shuvalov, V. A., Dekker, J. P., van Grondelle, R. & van Gorkom, H. J. (2004) *Biophys. J.* **86,** 1664–1672.
52. Müller, M. G., Niklas, J., Lubitz, W. & Holzwarth, A. R. (2003) *Biophys. J.* **85,** 3899–3922.
53. Holzwarth, A. R., Müller, M. G., Niklas, J. & Lubitz, W. (2006) *Biophys. J.* **90,** 552–565.
54. Schelvis, J. P. M., van Noort, P. I., Aartsma, T. J. & van Gorkom, H. J. (1992) in *Research in Photosynthesis*, ed. Murata, N. (Kluwer Academic, Dordrecht, The Netherlands), Vol. II, pp. 81–84.
55. Vacha, F., Joseph, D. M., Durrant, J. R., Telfer, A., Klug, D. R., Porter, G. & Barber, J. (1995) *Proc. Natl. Acad. Sci. USA* **92,** 2929–2933.
56. Konermann, L. & Holzwarth, A. R. (1996) *Biochemistry* **35,** 829–842.
57. Jankowiak, R., Rätsep, M., Picorel, R., Seibert, M. & Small, G. J. (1999) *J. Phys. Chem. B* **103,** 9759–9769.
58. Kuhl, H., Kruip, J., Seidler, A., Krieger-Liszkay, A., Bunker, M., Bald, D., Scheidig, A. J. & Rögner, M. (2000) *J. Biol. Chem.* **275,** 20652–20659.